PKC-induced Sensitization of Ca^{2+}-dependent Exocytosis Is Mediated by Reducing the Ca^{2+} Cooperativity in Pituitary Gonadotropes

Hua Yang,[1] Huisheng Liu,[1] Zhitao Hu,[1] Hongliang Zhu,[1] and Tao Xu[1,2]

[1]Institute of Biophysics and Biochemistry, School of Life Science and Technology, Huazhong University of Science and Technology, Wuhan 430074, P.R. China

[2]National Laboratory of Biomacromolecules, Institute of Biophysics, Chinese Academy of Sciences, Beijing 100101, P.R. China

ABSTRACT The highly cooperative nature of Ca^{2+}-dependent exocytosis is very important for the precise regulation of transmitter release. It is not known whether the number of binding sites on the Ca^{2+} sensor can be modulated or not. We have previously reported that protein kinase C (PKC) activation sensitizes the Ca^{2+} sensor for exocytosis in pituitary gonadotropes. To further unravel the underlying mechanism of how the Ca^{2+} sensor is modulated by protein phosphorylation, we have performed kinetic modeling of the exocytotic burst and investigated how the kinetic parameters of Ca^{2+}-triggered fusion are affected by PKC activation. We propose that PKC sensitizes exocytosis by reducing the number of calcium binding sites on the Ca^{2+} sensor (from three to two) without significantly altering the Ca^{2+}-binding kinetics. The reduction in the number of Ca^{2+}-binding steps lowers the threshold for release and up-regulates release of fusion-competent vesicles distant from Ca^{2+} channels.

KEY WORDS: exocytosis • kinetic modeling • Ca^{2+} dependency • fusion • protein phosphorylation

INTRODUCTION

Neuron and endocrine cells release neurotransmitters and hormones by highly regulated exocytosis of secretory vesicles. Calcium plays a pivotal role in triggering exocytosis. The relationship between the magnitude of Ca^{2+} entry and neurotransmitter release has been estimated to be approximately third order (Dodge and Rahamimoff, 1967; Augustine et al., 1985; Wu and Wu, 2001). Direct measurement of the relationship between the rate of exocytosis and the concentration of Ca^{2+} near release sites in a variety of neuron and endocrine cells has further supported the third- or fourth-order cooperative nature of Ca^{2+}-dependent exocytosis (Heidelberger et al., 1994; Xu et al., 1998; Schneggenburger and Neher, 2000; Voets, 2000; Beutner et al., 2001). This has been taken as indirect evidence that final Ca^{2+}-triggered fusion requires binding of at least three Ca^{2+} ions to the Ca^{2+} sensor(s).

It has been suggested that the fourth or higher order relationship between Ca^{2+} and exocytosis may be a unique feature of neuronal exocytosis, which is necessary for synchronizing neurotransmitter release with presynaptic Ca^{2+} influx. On the other hand, studies on hormone release from nonneuronal secretory cells have demonstrated a shallower dependence of exocytosis on Ca^{2+} of only second to third order, suggesting that variation in the number of Ca^{2+}-binding steps allows precise tuning of exocytosis. It has been shown that mutations in the surface residues of the soluble N-ethylmaleimide–sensitive factor attachment protein receptor (SNARE) complex cause a decrease in the number of sequential Ca^{2+}-binding steps preceding exocytosis (Sorensen et al., 2002). However, it is not known whether the number of binding sites on the Ca^{2+} sensor can be physiologically modulated or not.

Recently, we have shown that PKC activation sensitizes the Ca^{2+} sensor for exocytosis in pituitary gonadotropes (Zhu et al., 2002). To further uncover the underlying mechanism of how the Ca^{2+} sensor is modulated by phosphorylation, we have performed kinetic modeling of the experimental data and addressed the question of how the kinetic parameters for Ca^{2+} triggered exocytosis are influenced by PKC. We propose that PKC sensitizes exocytosis by reducing the number of calcium binding sites on the Ca^{2+} sensor from three to two, without significantly altering the Ca^{2+}-binding kinetics.

MATERIALS AND METHODS

Cell Culture and Solutions

Isolated gonadotropes were prepared as previously described (Zhu et al., 2002). In brief, the anterior pituitary was removed from 4- to 6-wk-old male Sprague–Dawley rats that had been castrated at week 2. Cells were used 2–4 d after dispersion. Experiments were done at room temperature in a bath solution containing 140 mM NaCl, 2.5 mM KCl, 1.3 mM $CaCl_2$, 1 mM $MgCl_2$, 10 mM Hepes, and 10 mM glucose (pH 7.4). Cells were

H. Yang and H. Liu contributed equally to this work.

Correspondence to Tao Xu: xutao@ibp.ac.cn

Abbreviations used in this paper: DMN, DM-nitrophen; HCSP, highly Ca^{2+}-sensitive pool; KS, Kolmogorov-Smirnov; NP-EGTA, nitrophenyl-EGTA.

J. Gen. Physiol. © The Rockefeller University Press • 0022-1295/2005/03/327/8 $8.00
Volume 125 March 2005 327–334
http://www.jgp.org/cgi/doi/10.1085/jgp.200409230

identified as gonadotropes as previously described (Kaftan et al., 2000). We confirmed our selection by challenging the cell with gonadotropin-releasing hormone (GnRH, 5 nM) and verifying a rapid, hormonally induced increase of in the intracellular free Ca^{2+} concentration ($[Ca^{2+}]_i$).

Membrane Capacitance (Cm) Measurement

Conventional whole-cell recordings used sylgard-coated 2–3 MΩ pipettes. Series resistances, which ranged from 4 to 12 MΩ, were included in the analysis. An EPC-9 patch-clamp amplifier was used together with PULSE+LOCK-IN software. A 977-Hz, 20-mV peak-to-peak sinusoidal voltage stimulus was superimposed on a holding potential of −80 mV. Currents were filtered at 2.9 kHz and sampled at 15.6 kHz.

Ca^{2+} Uncaging and $[Ca^{2+}]_i$ Measurement

Homogenous $[Ca^{2+}]_i$ elevation was generated by photolysis of caged Ca^{2+}, either nitrophenyl-EGTA (NP-EGTA) or DM-nitrophen (DMN). Flashes of UV light and fluorescence-excitation light were generated as described (Xu et al., 1997). The NP-EGTA–containing internal solutions consisted of 110 mM CsCl, 5 mM NP-EGTA, 2 mM NaCl, 4 mM $CaCl_2$, 2 mM MgATP, 0.3 mM GTP, 0.2 mM fura-6F, and 35 mM Hepes. To obtain a high level of postflash $[Ca^{2+}]_i$, we used DMN-containing internal solutions consisting of 110 mM CsCl, 10 mM DMN, 2 mM NaCl, 9 mM $CaCl_2$, 2 mM MgATP, 0.3 mM GTP, 0.2 mM furaptra, and 35 mM Hepes. The basal $[Ca^{2+}]_i$ was measured to be ~200 nM by fura-2. Internal solutions were adjusted to pH 7.2 with either HCl or CsOH. The $[Ca^{2+}]_i$ was calculated from the fluorescence ratio as previously described (Grynkiewicz et al., 1985).

To determine the $[Ca^{2+}]_i$ sensitivity of exocytosis, ramp $[Ca^{2+}]_i$ increases were generated by 5–10 s steady UV (380 nm) illumination (TILL Monochromator; TILL Photonics) of caged Ca^{2+}. The same light was also used to monitor $[Ca^{2+}]_i$ increases using the Ca^{2+} indicator, fura-6F. $[Ca^{2+}]_i$ was calculated as follows: $[Ca^{2+}]_i = Kd * (F\max - F)/(F - F\max/\beta)$, where $\beta = F\max/F\min$. *K*d of fura-6F is 5.3 μM as published by Molecular Probes. Because the basal $[Ca^{2+}]_i$ is buffered at ~200 nM, far below the *K*d of fura-6F, the initial fluorescence value can be used as *F*max. We neither measured the apparent *K*d of fura-6F under our conditions nor compensated for photobleaching.

Data Analysis and Modeling

Measured data were analyzed with IgorPro (Wavemetrics). The differential equations for models were solved using Igor's IntegrateODE function. The integrating routines were written and performed with IgorPro, compiled and run on Pentium PCs. For the fitting, we first assigned γ to either 120 s^{-1} for control cells, or 90 s^{-1} for cells pretreated with 100 nM PMA for 2–3 min, as determined from the experiment (see RESULTS for more details). The parameters α and β were then determined by fitting the experimental Cm trace to one of the kinetic models as shown in Scheme 1 and Scheme 2. By trial and error fitting, we found that α and β fluctuated around 14 $\mu M^{-1}s^{-1}$ and 51 s^{-1}, respectively. To avoid subjective fitting errors and to obtain the best fit, we adopted an objective criterion to assess the fitting; we varied α over the range 13–15 in 0.2 $\mu M^{-1}s^{-1}$ increments and β over the range 45–55 in 1 s^{-1} increments. We then calculated the square of the difference according to the following:

$$\sum w[i]\ (fit[i] - Cm[i])^2, \qquad (1)$$

where fit[i] is the calculated value according to the model for a given α and β pair, Cm[i] is the recorded raw Cm data, and w[i] is the corresponding weighting factor. Because the initial onset is sensitive to the Ca^{2+} stoichiometry, we set w[i] to 10 during the first 40 ms after the flash and 1 thereafter. The α and β pair that gave the minimal value according to Eq. 1 was considered the best fit. Values are given as the mean ± SEM. The Kolmogorov-Smirnov (KS) test was employed to assess the difference between cumulative histograms.

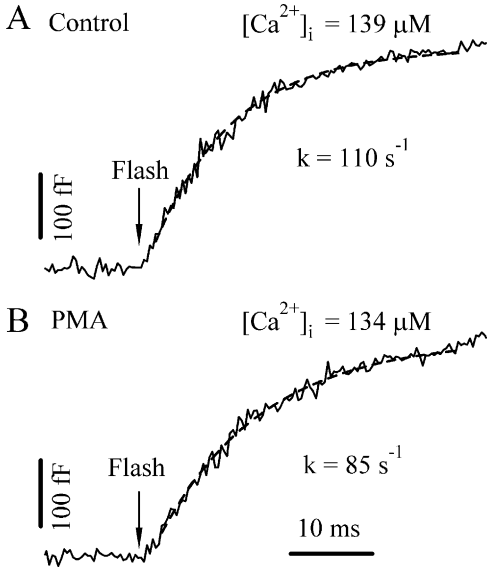

FIGURE 1. Determination of the irreversible fusion rate constant γ. We estimated γ by obtaining the rate constant for exocytosis from the single exponential fit of the initial burst component at very high postflash $[Ca^{2+}]_i$ levels. Two example Cm responses from a control (A) and a PMA-treated cell (B) are displayed. Dashed lines represent the fit to a single exponential.

RESULTS

In response to a stepwise elevation in $[Ca^{2+}]_i$ generated by flash photolysis of caged Ca^{2+}, exocytosis proceeds with an initial, rapid exocytotic burst followed by a slower, sustained phase (Thomas et al., 1993; Xu et al., 1999). The kinetics of the burst component is steeply dependent on $[Ca^{2+}]_i$. At higher $[Ca^{2+}]_i$, the rate constant of the burst becomes faster. Our previous studies have demonstrated that pretreatment with PMA (100 nM) for 2–3 min accelerates the exocytotic burst and lowers the $[Ca^{2+}]_i$ threshold required for exocytosis in gonadotropes. The effect of PMA was attributed to activation of PKC since it can be blocked by a specific PKC inhibitor and was not mimicked by an inactive phorbol ester analogue (Zhu et al., 2002). To better understand the mechanism of PKC action on the Ca^{2+}-sensing process of exocytosis, we performed kinetic modeling of the exocytotic burst. We started with a kinetic model (see Fig. 2 C, Scheme 1) including three equivalent Ca^{2+}-binding steps.

We first estimated the irreversible fusion rate constant, γ, by inducing high level postflash $[Ca^{2+}]_i$. The rate constant for exocytosis is expected to approach γ

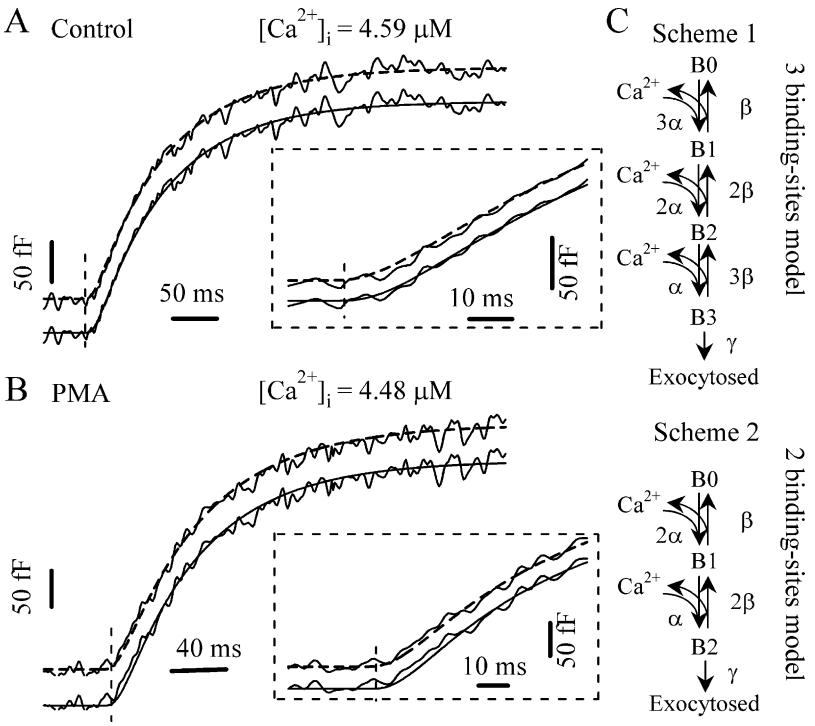

FIGURE 2. Fitting of the exocytotic responses to appropriate kinetic models. (A) Representative Cm response from a control cell. The best fit was obtained using a three-step binding model (Scheme 1) giving the parameters $\alpha = 14\ \mu M^{-1}s^{-1}$, $\beta = 51\ s^{-1}$, and $\gamma = 120\ s^{-1}$ (solid line). The initial onset of the response after the flash is expanded in the inset to show the sigmoidal region in detail. The fit to a two-step binding model (Scheme 2) gives $\alpha = 8.8\ \mu M^{-1}s^{-1}$, $\beta = 52\ s^{-1}$, and $\gamma = 120\ s^{-1}$ (dashed line). (B) Cm response from a PMA-treated cell. The best fit to the model of Scheme 2 (dashed line) gives $\alpha = 14\ \mu M^{-1}s^{-1}$, $\beta = 51\ s^{-1}$, and $\gamma = 90\ s^{-1}$. Inset, comparison of the fits to Scheme 1 (solid line, $\alpha = 21.8\ \mu M^{-1}s^{-1}$, $\beta = 50\ s^{-1}$, $\gamma = 90\ s^{-1}$) and Scheme 2 for the initial onset. (C) Sequential Ca^{2+}-binding models for exocytosis. (Top) Scheme 1 model with three equivalent Ca^{2+}-binding sites. (Bottom) Scheme 2 model with only two equivalent Ca^{2+}-binding sites.

at very high $[Ca^{2+}]_i$. We obtained the rate constants for exocytosis by fitting the burst component to a single exponential. The rate constants displayed a steep dependence on $[Ca^{2+}]_i$ and ranged from 95 to 116 s^{-1} when the $[Ca^{2+}]_i$ exceeded 100 μM (one example is shown in Fig. 1 A, see also Fig. 5 A). We therefore set the parameter γ to 120 s^{-1} accordingly, which is ~5% more than the experimental range to be sure that γ is not underestimated. This number is ~10-fold lower than that for chromaffin cells (Sorensen, 2004), but is consistent with previous findings in gonadotropes (Tse et al., 1997), probably reflecting a difference in the secretory machinery involved in the final fusion. Interestingly, we found the rate constants for exocytosis at higher $[Ca^{2+}]_i$ after PMA treatment were consistently smaller than those for the control cells. The rate constants for PMA-treated cells ranged from 70 to 85 s^{-1} when the $[Ca^{2+}]_i$ exceeded 100 μM (one example is shown in Fig. 1 B, see also Fig. 5 A). Hence, the parameter γ was set to 90 s^{-1} for PMA-treated cells.

After determining the parameter γ for control and PMA-treated cells, we next fitted the experimental responses to determine the rest of the parameters for the kinetic model(s). We found that the Cm responses to flash photolysis from control cells fit quite well to the model shown in Fig. 2 C, Scheme 1, giving values of around 14 $\mu M^{-1}\cdot s^{-1}$ and 51 s^{-1} for α and β, respectively. Using a kinetic model with two equivalent Ca^{2+} binding steps (Fig. 2 C, Scheme 2) also yielded a reasonable fit to the traces for the overall time course of the burst component, albeit with lower α values. The exocytotic burst component always starts with a lag, resulting in a sigmoidal appearance of the Cm trace. It has been suggested that the binding of multiple Ca^{2+} ions contributes to this lag. Closer inspection of the onset of the response immediately after the flash shows that a model with three Ca^{2+}-binding steps reproduces the sigmoidicity better than the model with two Ca^{2+}-binding steps (Fig. 2 A, inset). To fit the Cm responses in the presence of PMA, we had to choose higher α values when using Scheme 1 (Fig. 2 B). However, when fitting the PMA-treated responses with two Ca^{2+}-binding steps, similar α and β values were obtained as those for control responses when the three-step Ca^{2+}-binding model was used. Also, the model with two Ca^{2+}-binding steps seems to better describe the less sigmoidal feature of the onset of the PMA-treated responses, as shown in the inset of Fig. 2 B.

Clearly, it is not possible to exclude any particular Ca^{2+} stoichiometry from subtle difference in the fits to the onset of the flash responses. We therefore fitted all the experimental responses to both Scheme 1 and 2. The α and β values obtained are plotted in Fig. 3. The α values from 81 control cells display a narrow Gaussian distribution with a peak at 13.8 $\mu M^{-1}\cdot s^{-1}$ when a three-step Ca^{2+} binding model (Scheme 1) was used, which is in contrast to the broader distribution of α when Scheme 2 was used (Fig. 3 A). This difference is significant ($P < 0.01$, KS test) when comparing the cumulative histogram plot. In contrast, in the presence of PMA, the estimated values for α using Scheme 1 displayed a broader distribution with a less clear peak

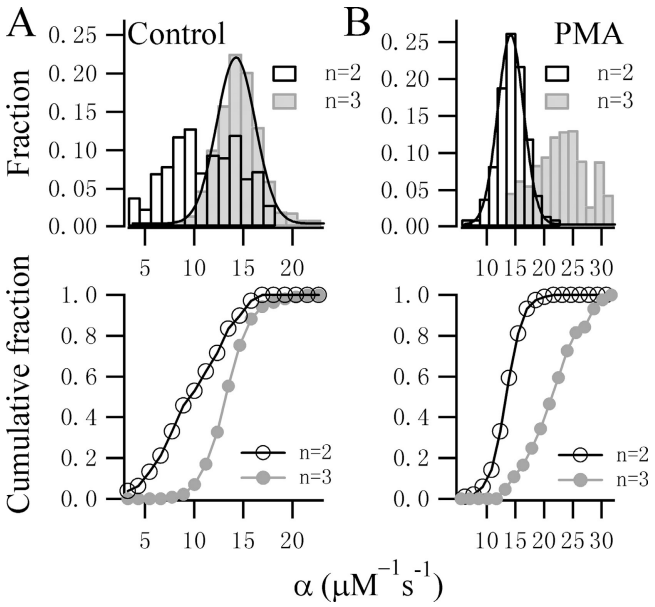

FIGURE 3. Comparison of the fitting results for control and PMA-treated traces using different Ca^{2+}-binding models. (A) The distribution and cumulative histogram of α values obtained from the fits for 81 control cells using Scheme 1 (gray bars) or Scheme 2 (open bars). Using Scheme 1, the distribution of α values displayed a sharp Gaussian distribution with a peak at 13.8 $\mu M^{-1}s^{-1}$ and a variation of 2.0 $\mu M^{-1}s^{-1}$, but was more broad when fitting to a model for only two Ca^{2+}-binding sites. The difference in the two datasets is significant (KS test, $P < 0.01$). (B) The distribution and cumulative histogram of α values obtained from the fits for 95 PMA-treated traces using Scheme 1 (gray symbols) or Scheme 2 (open symbols). The distribution of α values showed a sharp Gaussian function for the model assuming two Ca^{2+}-binding steps with a peak at 14.2 $\mu M^{-1}s^{-1}$ and a variation of 2.3 $\mu M^{-1}s^{-1}$.

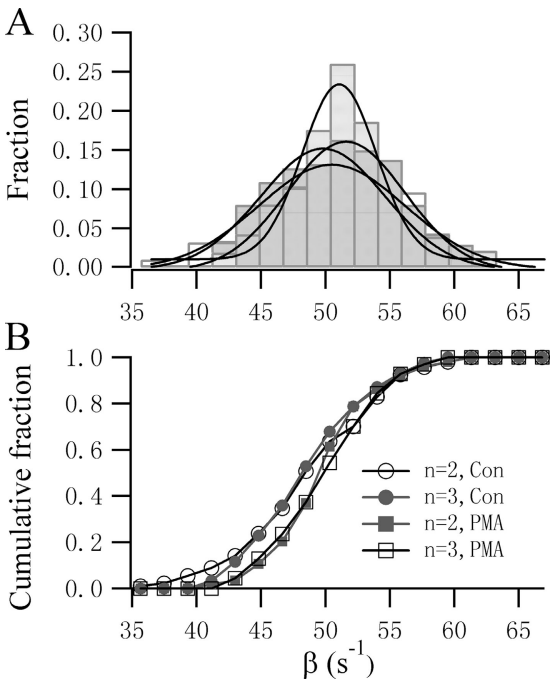

FIGURE 4. The value of β is not sensitive to the Ca^{2+} stoichiometry of the model chosen. The distribution (top) and the cumulative histogram (bottom) of β values obtained from the fits to two-step and three-step models was not significantly different (KS test, $P > 0.05$) for either control or PMA-treated cells. Gaussian fits to the four groups of β values yield similar peaks varying from 49.8 s^{-1} to 51.6 s^{-1}.

(Fig. 3 B). When Scheme 2 was used to fit the data, a narrow Gaussian distribution of α was obtained with a clear peak at 14.2 $\mu M^{-1}\cdot s^{-1}$. This difference is also clear from the cumulative histogram plot. Interestingly, the β value is less sensitive to the Ca^{2+} stoichiometry and follows a Gaussian distribution with a peak around 51 s^{-1} regardless of the number of Ca^{2+}-binding steps chosen (Fig. 4). Similarly, no significant difference was observed in the cumulative histogram plots as assessed by KS test.

We then examined whether our choice of Ca^{2+} stoichiometry and the kinetic parameters obtained could describe the observed Ca^{2+}-dependent features of exocytosis. For this purpose, we plotted the rate constants of the burst components versus postflash $[Ca^{2+}]_i$. By assigning three Ca^{2+}-binding steps (Scheme 1) for control cells and two Ca^{2+}-binding steps (Scheme 2) for PMA-treated cells, we observed good accordance of the predicted and measured Ca^{2+} dependence of the rate constants for the burst component (Fig. 5 A). As explained above, the sigmoidal delay after the flash is another indication that multiple Ca^{2+}-binding steps are required in order to trigger fusion. A higher degree of cooperativity results in a more strongly sigmoidal feature with a longer delay, whereas lower cooperativity usually results in an instantaneous response. We examined the dependence of the delay on $[Ca^{2+}]_i$ and found that cells treated with PMA have a consistently shorter delay. The delay as a function of $[Ca^{2+}]_i$ also fits well to the three and two Ca^{2+}-binding stoichiometry for control and PMA-treated cells, respectively (Fig. 5 B).

To further confirm the modulatory mechanism of PMA on Ca^{2+} sensing, we employed the so-called "Ca^{2+} ramp" technique, where Ca^{2+} is liberated slowly from the caged Ca^{2+} over the course of 2–5 s by steady UV illumination. Since the K_d of a single Ca^{2+} binding reaction is calculated to be around 4 μM, a Ca^{2+} ramp from several hundred nM to a few μM will be ideal for this purpose because the Ca^{2+} sensor is far from saturation over this range. The derivation of Ca^{2+} dependence of exocytosis from single ramp stimulation also minimizes cell-to-cell variation. The Cm responses to a Ca^{2+} ramp for control and PMA-treated cells are displayed in Fig. 6 (A and B). Based on the calculation of the local rate of the Cm change and the estimate of the size of the releasable pool, we calculated the rate of the release at different $[Ca^{2+}]_i$ levels. Fig. 6 C compares the averaged

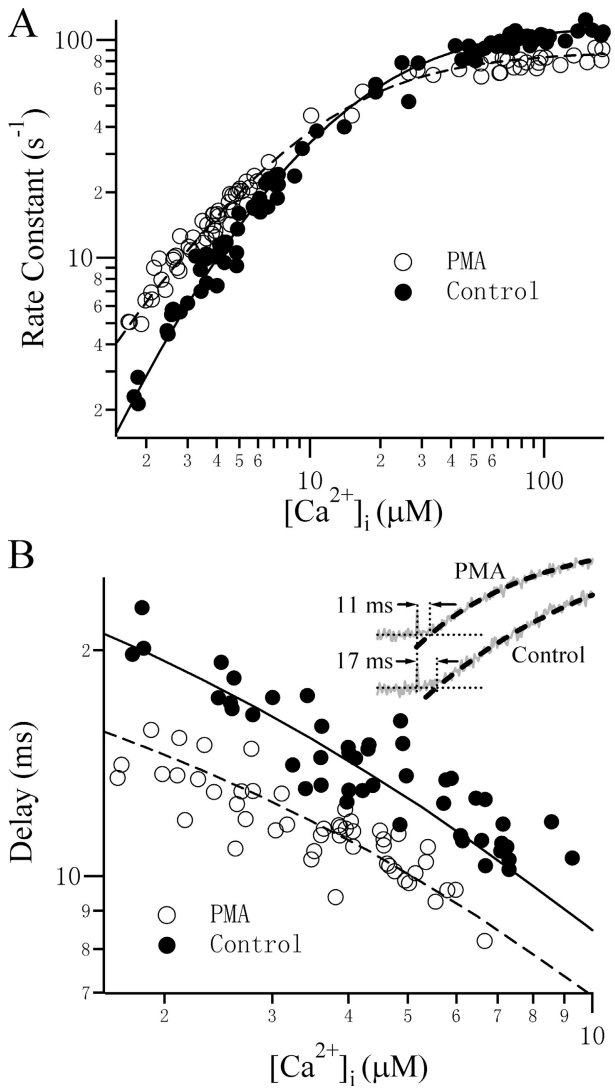

FIGURE 5. The Ca^{2+} dependence of the kinetics of exocytosis can be described by models with the appropriate number of Ca^{2+}-binding sites. Rate constants (A) and the delays (B) for control (filled circles) and PMA-treated (open circles) cells were plotted as a function of the postflash $[Ca^{2+}]_i$ level. Lines represent the simulated values using Scheme 1 (solid lines, $\alpha = 14\ \mu M^{-1}s^{-1}$, $\beta = 51\ s^{-1}$, $\gamma = 120\ s^{-1}$) and Scheme 2 (dashed lines, $\alpha = 14\ \mu M^{-1}s^{-1}$, $\beta = 51\ s^{-1}$, $\gamma = 90\ s^{-1}$). The delay was defined as the time interval between the flash and the time point at which the fitted curve (dashed line) crosses the preflash Cm level (Inset). From this value, 0.6 ms was subtracted to account for the delay required for Ca^{2+} to be released from the caged Ca^{2+}. The postflash $[Ca^{2+}]_i$ levels are 3.40 μM and 3.22 μM for the Control and PMA-treated cells, respectively.

rate of release from control and PMA-treated cells as a function of $[Ca^{2+}]_i$ on a double logarithmic scale. It is evident that although PMA-treated cells exhibit larger rate constants, they have a shallower dependence on $[Ca^{2+}]_i$. The slope was 2.7 for control and 1.6 for PMA-treated cells. A satisfactory fit to the mean control data (Fig. 6 C, lower solid line) was achieved using Scheme 1 with the same kinetic parameters used in Fig. 5. To account for the shallower slope of the PMA-treated cells, we had to reduce the number of Ca^{2+}-binding sites by one, as in Scheme 2, in order to yield a satisfactory fit (Fig. 6 C, upper dashed line). The time courses of the Cm response to a Ca^{2+} ramp also fitted well to Scheme 1 for control (Fig. 6 A, dashed line) and Scheme 2 for PMA-treated cells (Fig. 6 B, dashed line).

DISCUSSION

In the present study, we have taken advantage of the photolysis technique to elevate $[Ca^{2+}]_i$ homogeneously and to study the relationship between the concentration of Ca^{2+} and the kinetics of exocytosis. The results obtained by fitting the experimental data to appropriate kinetic models for exocytosis suggest that sensitization of the secretory machinery by PKC phosphorylation involves reduction of the number of Ca^{2+}-binding sites on the Ca^{2+} sensor for exocytosis without altering its binding kinetics.

PMA has been demonstrated to facilitate neurotransmitter release (Stevens and Sullivan, 1998; Yawo, 1999; Wu and Wu, 2001) as well as hormone secretion in endocrine cells (Ammala et al., 1994; Gillis et al., 1996; Billiard et al., 1997). The rate of release is proportional to the product of the size of the readily releasable pool (RRP) multiplied by the average probability of release. PMA has been suggested to augment the RRP size in both neurons (Stevens and Sullivan, 1998) and endocrine cells (Gillis et al., 1996). However, evidence has accumulated recently that PMA can also increase the probability of release by inducing the appearance of a highly Ca^{2+}-sensitive pool (HCSP) of vesicles in a number of cell types (Yang et al., 2002; Zhu et al., 2002; Wan et al., 2004; Yang and Gillis, 2004). The steep dependence (third to fourth power) of exocytosis on $[Ca^{2+}]_i$ means that even a small change in Ca^{2+} sensitivity could have large effects on the release rate. Indeed, our previous work has suggested that a twofold increase in the Ca^{2+} sensitivity of exocytosis caused by PMA predicts an approximately eightfold increase in the release rate at resting $[Ca^{2+}]_i$, similar to what has been previously reported (Billiard, et al., 1997). Although sensitization of the secretory machinery is regarded as a powerful way of augmenting the release, the mechanism underlying the sensitization (or the transition to HCSP) is unclear. We observed that the relationship between the rate of exocytosis of vesicles in the HCSP and the postflash $[Ca^{2+}]_i$ after PMA treatment is not as steep as in control gonadotropes. Further analysis of the kinetics of exocytosis revealed that while a model incorporating three independent Ca^{2+}-binding steps preceding the final fusion step is required to describe the control data, it could not adequately describe the HCSP after PMA treatment. Rather, the relatively shal-

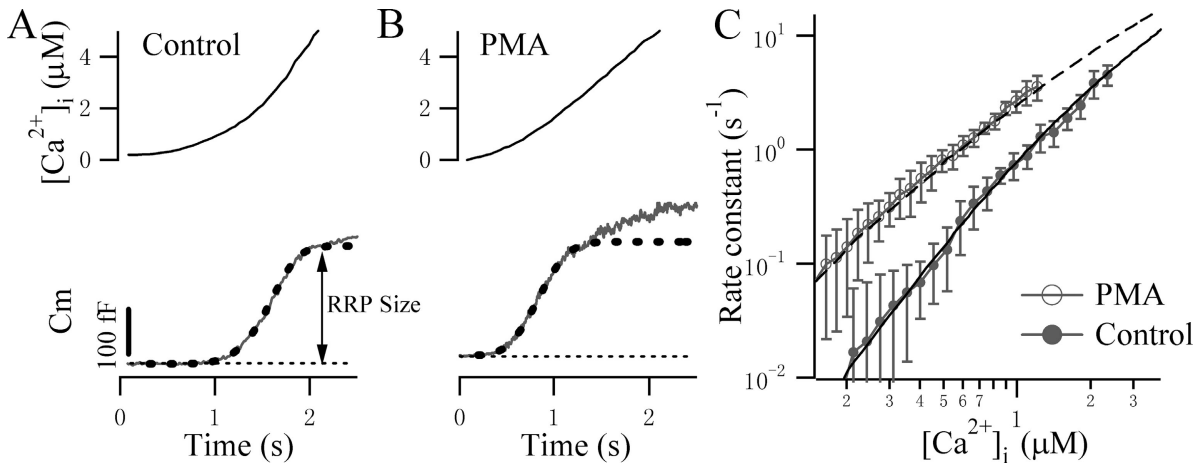

FIGURE 6. PMA treatment reduces the steepness of the Ca^{2+} dependence of exocytosis revealed by ramp $[Ca^{2+}]_i$ stimulation. Example Cm responses of a control (A) and PMA-treated (B) cells stimulated by ramp $[Ca^{2+}]_i$. The smooth dashed lines represent simulated responses using the models shown in Schemes 1 and 2 in the absence and presence of PMA, respectively. (C) Double logarithmic plot of the rate constants versus $[Ca^{2+}]_i$ for 10 control (open circles) and 7 PMA-treated (filled circles) cells. The local rate constant was calculated as the exocytotic rate divided by the remaining pool size. The slope was 2.7 for the control and 1.6 for PMA-treated cells. Using the measured ramp $[Ca^{2+}]_i$ as a forcing function, the control data were fitted to a three-step Ca^{2+}-binding model (Scheme 1), whereas the PMA data were fitted to the two-step Ca^{2+}-binding model (Scheme 2).

low dependence of the rate constant for exocytosis on $[Ca^{2+}]_i$ can be best modeled by two Ca^{2+}-binding steps. Another finding of this study is that sensitization of the Ca^{2+} sensor by PMA is not associated with changes in the binding and dissociation kinetics of the Ca^{2+} to independent binding sites. By choosing kinetic models with appropriate Ca^{2+} stoichiometry, we found that the rate constants obtained from the fits, α and β, converged to the values 14 $\mu M^{-1} \cdot s^{-1}$ and 51 s^{-1}, respectively, regardless of whether PMA was present. Adequate measurement of these parameters has only been performed in chromaffin cells. Interestingly, we found that the value of β is not sensitive to the Ca^{2+} stoichiometry chosen and is almost identical to that estimated previously for chromaffin cells ($\beta = 56\ s^{-1}$; Voets, 2000). The value of α in gonadotropes is slightly higher than that for chromaffin cells and probably reflects the involvement of a higher affinity Ca^{2+} sensor in gonadotropes. In contrast, the value of γ in gonadotropes is much lower than that of the so-called rapidly releasable pool but comparable to that of the slowly releasable pool in chromaffin cells (Voets, 2000). Mutations in SNARE complexes also greatly reduce the value of γ without any apparent influence on the value of α and β (Sorensen et al., 2002). Interestingly, we found that PMA treatment slightly reduced the value of γ. The rate constants of exocytosis of control and PMA-treated cells actually crossed at a $[Ca^{2+}]_i$ level of 14 μM as predicted from the model (Fig. 5 A). Thus, the effect of PMA on the kinetics of exocytosis can only be observed at low $[Ca^{2+}]_i$ levels (i.e., a few μM). In contrast, at higher $[Ca^{2+}]_i$, it is not possible to distinguish any effect of PMA on the kinetics of exocytosis. Rather, the rate constants of exocytosis from PMA-treated cells should be slightly lower than that for control cells. This explains why a previous study using high postflash $[Ca^{2+}]_i$ failed to detect any influence of PMA on the kinetics of the burst component (Gillis et al., 1996).

The fourth- to fifth-order dependence of exocytosis on $[Ca^{2+}]_i$ is thought to be important for the characteristics of synchronous release. It also restricts the release sites to the Ca^{2+} entry sites. In contrast, the second- to third-order dependence of the rate of release on $[Ca^{2+}]_i$ is consistent with the less demanding role of synchronization of hormone release from secretory cells. The reduction in the number of Ca^{2+}-binding steps by PMA would further lower the threshold for release and tune the Ca^{2+} sensor to spatially averaged $[Ca^{2+}]_i$ rather than nonoverlapping Ca^{2+} microdomains. Thus, more vesicles distant from Ca^{2+}-channels will be released. Indeed, the majority of the RRP is found distant from the vicinity of Ca^{2+} channels in a number of endocrine cell types, including gonadotropes, chromaffin cells, and β cells (Moser and Neher, 1997; Voets, 2000; Barg et al., 2001; Yang et al., 2002; Zhu et al., 2002). Decreasing the order of $[Ca^{2+}]_i$ dependence of release provides an efficient way of promoting release in these cells. In fact, a high affinity/low cooperativity exocytosis has been demonstrated in rod photoreceptors, permitting rods to respond linearly to the change of Ca^{2+} influx due to graded light responses (Thoreson et al., 2004). Sensitization of the Ca^{2+} sensor for exocytosis without apparent modulation of the RRP size has been suggested to occur in

both endocrine cells (Yang et al., 2002; Zhu et al., 2002; Wan et al., 2004; Yang and Gillis, 2004) and neurons (Yawo 1999; Wu and Wu, 2001). The mechanism described in this study may thus apply to both endocrine cells and neurons. This is quite likely, as both these cell types utilize similar molecules in priming and fusion.

The targets of PMA action remain to be explored. Besides PKC, Munc13 has been suggested recently as an important receptor for phorbol esters. It is now believed that Munc13 is essential for the priming of vesicles by activating syntaxin in an open conformation (Brose et al., 2000; Silinsky and Searl, 2003; Junge et al., 2004). Activated syntaxin thus initiates the assembly of the primed core complex that makes vesicles fusion competent (Xu et al., 1999). It is suggested that the augmentation of neurotransmitter release by phorbol esters in hippocampal neurons might actually be due to the effects on Munc13 (Rhee et al., 2002). Binding of the C1 domain of Munc13 by phorbol esters is suggested to facilitate the priming and thus increase the RRP size. We have shown that the effect of PMA on the Ca^{2+} sensitivity of exocytosis is blocked by the PKC-specific inhibitor BIS, which binds to the ATP-binding domain (C3) of PKC. In contrast, Munc13 lacks a C3 domain. Moreover, the modulation we describe here applies to the final Ca^{2+}-sensing steps of fusion, which is distinct from an effect on the RRP size caused by activation of Munc13. Thus, our results seem to point to a novel target of action, distinct from Munc13. Synaptotagmin has been proposed as the major Ca^{2+} sensor that mediates fusion, yet the precise mechanism of Ca^{2+} binding and the subsequent fusogenic action is unknown. The cytoplasmic region of synaptotagmin contains two C2 domains, C2A and C2B. It has been suggested that five highly conserved acidic residues in both the C2A and C2B domains coordinate the binding of three to four Ca^{2+} ions (Chapman et al., 2002; Sudhof, 2002). However, evidence also suggests that other auxiliary proteins may be involved in the Ca^{2+}-sensing step. For instance, mutations in SNARE proteins change the calcium sensitivity and reduce the Ca^{2+} dependence of exocytosis in chromaffin cells, suggesting that the SNARE complex and synaptotagmin might constitute an integrated Ca^{2+} sensor for fusion. Indeed, double mutations in the two acidic and hydrophilic residues in the COOH-terminal end of SNAP-25, which has been postulated to coordinate divalent ion binding from the crystallized core SNARE complex, reduced the slope of Ca^{2+} dependence of exocytosis from 2.7 to 1.5, without significantly changing the Ca^{2+}-binding kinetics (Sorensen et al., 2002). This result is in close agreement the PMA effect we observed in this study. It is not yet known whether an additional, unknown partner is required for the structural integrity of the Ca^{2+}-binding sites, in which case phosphorylation of the auxiliary proteins of the Ca^{2+}-sensing complex may lead to the loss of a Ca^{2+}-binding site. Further experiments will be needed to elucidate the underlying mechanism of this modulation of the Ca^{2+}-sensing steps that immediately precede the final fusion.

We thank Drs. Sarah Perrett and Bertil Hille for critical reading of the manuscript.

This work was supported by grants from the National Science Foundation of China (30025023, 30270363, 30130230, 30470448), the Major State Basic Research Program of P.R. China (G1999054000, 2004CB720000), the CAS Project (KSCX2-SW-224), the Li Foundation, and the Sino-German Scientific Center. The laboratory of T. Xu belongs to a Partner Group Scheme of the Max Planck Institute for Biophysical Chemistry, Göttingen.

Angus C. Nairn served as editor.

Submitted: 6 December 2004
Accepted: 18 January 2005

REFERENCES

Ammala, C., L. Eliasson, K. Bokvist, P.O. Berggren, R.E. Honkanen, A. Sjoholm, and P. Rorsman. 1994. Activation of protein kinases and inhibition of protein phosphatases play a central role in the regulation of exocytosis in mouse pancreatic beta cells. *Proc. Natl. Acad. Sci. USA*. 91:4343–4347.

Augustine, G.J., M.P. Charlton, and S.J. Smith. 1985. Calcium entry and transmitter release at voltage-clamped nerve terminals of squid. *J. Physiol.* 367:163–181.

Barg, S., X. Ma, L. Eliasson, J. Galvanovskis, S.O. Gopel, S. Obermuller, J. Platzer, E. Renstrom, M. Trus, D. Atlas, et al. 2001. Fast exocytosis with few Ca^{2+} channels in insulin-secreting mouse pancreatic B cells. *Biophys. J.* 81:3308–3323.

Beutner, D., T. Voets, E. Neher, and T. Moser. 2001. Calcium dependence of exocytosis and endocytosis at the cochlear inner hair cell afferent synapse. *Neuron*. 29:681–690.

Billiard, J., D.S. Koh, D.F. Babcock, and B. Hille. 1997. Protein kinase C as a signal for exocytosis. *Proc. Natl. Acad. Sci. USA*. 94: 12192–12197.

Brose, N., C. Rosenmund, and J. Rettig. 2000. Regulation of transmitter release by Unc-13 and its homologues. *Curr. Opin. Neurobiol.* 10:303–311.

Chapman, A.L., M.B. Hampton, R. Senthilmohan, C.C. Winterbourn, and A.J. Kettle. 2002. Chlorination of bacterial and neutrophil proteins during phagocytosis and killing of *Staphylococcus aureus*. *J. Biol. Chem.* 277:9757–9762.

Dodge, F.A., Jr., and R. Rahamimoff. 1967. Co-operative action a calcium ions in transmitter release at the neuromuscular junction. *J. Physiol.* 193:419–432.

Gillis, K.D., R. Mossner, and E. Neher. 1996. Protein kinase C enhances exocytosis from chromaffin cells by increasing the size of the readily releasable pool of secretory granules. *Neuron*. 16: 1209–1220.

Grynkiewicz, G., M. Poenie, and R.Y. Tsien. 1985. A new generation of Ca^{2+} indicators with greatly improved fluorescence properties. *J. Biol. Chem.* 260:3440–3450.

Heidelberger, R., C. Heinemann, E. Neher, and G. Matthews. 1994. Calcium dependence of the rate of exocytosis in a synaptic terminal. *Nature*. 371:513–515.

Junge, H.J., J.S. Rhee, O. Jahn, F. Varoqueaux, J. Spiess, M.N. Waxham, C. Rosenmund, and N. Brose. 2004. Calmodulin and Munc13 form a Ca^{2+} sensor/effector complex that controls short-term synaptic plasticity. *Cell*. 118:389–401.

Kaftan, E.J., T. Xu, R.F. Abercrombie, and B. Hille. 2000. Mitochondria shape hormonally induced cytoplasmic calcium oscillations and modulate exocytosis. *J. Biol. Chem.* 275:25465–25470.

Moser, T., and E. Neher. 1997. Rapid exocytosis in single chromaffin cells recorded from mouse adrenal slices. *J. Neurosci.* 17:2314–2323.

Rhee, J.S., A. Betz, S. Pyott, K. Reim, F. Varoqueaux, I. Augustin, D. Hesse, T.C. Sudhof, M. Takahashi, C. Rosenmund, and N. Brose. 2002. Beta phorbol ester- and diacylglycerol-induced augmentation of transmitter release is mediated by Munc13s and not by PKCs. *Cell.* 108:121–133.

Schneggenburger, R., and E. Neher. 2000. Intracellular calcium dependence of transmitter release rates at a fast central synapse. *Nature.* 406:889–893.

Silinsky, E.M., and T.J. Searl. 2003. Phorbol esters and neurotransmitter release: more than just protein kinase C? *Br. J. Pharmacol.* 138:1191–1201.

Sorensen, J.B., U. Matti, S.H. Wei, R.B. Nehring, T. Voets, U. Ashery, T. Binz, E. Neher, and J. Rettig. 2002. The SNARE protein SNAP-25 is linked to fast calcium triggering of exocytosis. *Proc. Natl. Acad. Sci. USA.* 99:1627–1632.

Sorensen, J.B. 2004. Formation, stabilisation and fusion of the readily releasable pool of secretory vesicles. *Pflugers Arch.* 448: 347–362.

Stevens, C.F., and J.M. Sullivan. 1998. Regulation of the readily releasable vesicle pool by protein kinase C. *Neuron.* 21:885–893.

Sudhof, T.C. 2002. Synaptotagmins: why so many? *J. Biol. Chem.* 277: 7629–7632.

Thomas, P., J.G. Wong, A.K. Lee, and W. Almers. 1993. A low affinity Ca^{2+} receptor controls the final steps in peptide secretion from pituitary melanotrophs. *Neuron.* 11:93–104.

Thoreson, W.B., K. Rabl, E. Townes-Anderson, and R. Heidelberger. 2004. A highly Ca^{2+}-sensitive pool of vesicles contributes to linearity at the rod photoreceptor ribbon synapse. *Neuron.* 42: 595–605.

Tse, F.W., A. Tse, B. Hille, H. Horstmann, and W. Almers. 1997. Local Ca^{2+} release from internal stores controls exocytosis in pituitary gonadotrophs. *Neuron.* 18:121–132.

Voets, T. 2000. Dissection of three Ca^{2+}-dependent steps leading to secretion in chromaffin cells from mouse adrenal slices. *Neuron.* 28:537–545.

Wan, Q.F., Y.M. Dong, H. Yang, X.L. Lou, J.P. Ding, and T. Xu. 2004. Protein kinase activation increases insulin secretion by sensitizing the secretory machinery to Ca^{2+}. *J. Gen. Physiol.* 124:653–662.

Wu, X.S., and L.G. Wu. 2001. Protein kinase c increases the apparent affinity of the release machinery to Ca^{2+} by enhancing the release machinery downstream of the Ca^{2+} sensor. *J. Neurosci.* 21: 7928–7936.

Xu, T., M. Naraghi, H. Kang, and E. Neher. 1997. Kinetic studies of Ca^{2+} binding and Ca^{2+} clearance in the cytosol of adrenal chromaffin cells. *Biophys. J.* 73:532–545.

Xu, T., T. Binz, H. Niemann, and E. Neher. 1998. Multiple kinetic components of exocytosis distinguished by neurotoxin sensitivity. *Nat. Neurosci.* 1:192–200.

Xu, T., B. Rammner, M. Margittai, A.R. Artalejo, E. Neher, and R. Jahn. 1999. Inhibition of SNARE complex assembly differentially affects kinetic components of exocytosis. *Cell.* 99:713–722.

Yang, Y., S. Udayasankar, J. Dunning, P. Chen, and K.D. Gillis. 2002. A highly Ca^{2+}-sensitive pool of vesicles is regulated by protein kinase C in adrenal chromaffin cells. *Proc. Natl. Acad. Sci. USA.* 99: 17060–17065.

Yang, Y., and K.D. Gillis. 2004. A highly Ca^{2+}-sensitive pool of granules is regulated by glucose and protein kinases in insulin–secreting INS-1 cells. *J. Gen. Physiol.* 124:641–651.

Yawo, H. 1999. Protein kinase C potentiates transmitter release from the chick ciliary presynaptic terminal by increasing the exocytotic fusion probability. *J. Physiol.* 515(Pt 1):169–180.

Zhu, H.L., B. Hille, and T. Xu. 2002. Sensitization of regulated exocytosis by protein kinase C. *Proc. Natl. Acad. Sci. USA.* 99:17055–17059.